Intermetallics 75 (2016) 36–41

Contents lists available at ScienceDirect

Intermetallics

journal homepage: www.elsevier.com/locate/intermet

Intrinsic structural defects on medium range in metallic glasses

X. Huang [a], Z. Ling [b], Y.J. Wang [b], L.H. Dai [b, *]

[a] Institute of Systems Engineering, China Academy of Engineering Physics, Mianyang, Sichuan 621999, China
[b] State Key Laboratory of Nonlinear Mechanics, Institute of Mechanics, Chinese Academy of Sciences, Beijing 100190, China

ARTICLE INFO

Article history:
Received 6 March 2016
Received in revised form
5 May 2016
Accepted 26 May 2016

Keywords:
Metallic glasses
Structural defects
Medium range order

ABSTRACT

To get insight into the structural defects on medium range in metallic glasses, molecular dynamic simulations on cavitation instability are carried out. It is found that micro voids are prone to nucleate at the sites where atomic clusters are loose packing on medium range. Close-up observation on atomic clusters around the nucleation site shows that there are two kinds of defects on medium range: cavities among the atomic clusters and boundaries between medium range orders. Further investigation shows that the defects are significantly important in both cavitation and shear transformation, which are two intrinsic deformation modes of metallic glasses.

1. Introduction

Intrinsic structural defects such as vacancies, dislocations and grain boundaries, usually play important roles in the mechanical behaviors of conventional crystalline materials. For example, plastic deformation is attributed to the motion of dislocations, and damage evolution process which leads to catastrophic failure is usually due to vacancy clustering, dislocation pileup, grain boundary sliding, etc. [1] In contrast, in metallic glasses (MGs) [2,3] which are relatively new kind of materials and exhibit excellent physical and mechanical properties, what the intrinsic structural defects are and how they influence the material properties still fascinates and challenges scientists.

MGs are amorphous metastable solids which are usually made by fast quenching process. For the unique disordered structures, MGs are lack of long-range translational order and have long-range homogeneity. Thus, unlike their crystalline counterparts, heterogeneities on mesoscopic scale do not exist in MGs and their properties are significantly influenced by atomic structures on microscopic scale [4–11]. To characterize the atomic-level structure of MGs, much work has been done over the past few decades [12–23]. The atomic structure of MGs are initially described as dense random packing of hard spheres [12]. Now it is widely accepted that they have short-range orders (SROs), which is constituted by the atomic configuration of the nearest-neighbor shell, contributing to the first peak in the pair distribution function (PDF) [4,13]. They are the basic building blocks [14] characterized by different types of polyhedra, and icosahedral (or icosahedral-like) order is the most favourable local order [16–18]. Recently, medium-range orders (MROs) have been found to exist in MGs too. The dense packing of atomic clusters by sharing shell atoms (face sharing, edge sharing, or vertex sharing) forms MRO [20,24–27], thus the structural features are beyond the first peak in PDF to a distance up to 1–2 nm. Further investigation shows that the packing of clusters may be characterized as fractals [28,29]. Furthermore, on a length scale beyond MROs, the material is believed to consist of hard matrix and soft zones (or liquid-like regions) [10,11,23]. The hard matrix, which is rich in interpenetrating icosahedral-like orders, are the backbone of MGs. Soft zones, which contain disordered clusters with low packing efficiency, are regarded as heterogeneities.

The above works established a relatively clear picture of structural organization in MGs, but the defects in such kind of material are far from being understood. It is well known that there are no vacancies, dislocations or grain boundaries in MGs. Free volume [30] and disclinations [31] are believed to be the structural defects. Free volume is the “flow defect”, which can be described as local fluctuations of density. Disclinations are rotational defects, usually seen as sixfold and fourfold bipyramids. Now these concepts are widely used to understand the mechanical and physical behavior of MGs [32–39]. However, all of them can be regarded as defects on short range. As there are MROs which determine cluster packing over a longer length scale, they may be as important as SROs in

* Corresponding author.
E-mail address: lhdai@lnm.imech.ac.cn (L.H. Dai).

http://dx.doi.org/10.1016/j.intermet.2016.05.009
0966-9795/

affecting the material properties [4]. Then, are there any structural defects on medium range? How do they act during the deformation and failure processes of MGs [40–42]?

In this work, cavitation instability [43] in a binary metallic glass (MG) $Cu_{50}Zr_{50}$ is studied via dynamic molecular (MD) simulations. To characterize the intrinsic structural defects, micro-structure evolution under tensile pressure is analyzed, with special attention on evolution of the atomic clusters around void nucleation sites. The physical picture of intrinsic structural defects on medium range is presented, and the role that the defects play in cavitation process is discussed. Besides, via additional simulations on compression of the material, we also show how the shear transformation event is mediated by the defects. Thus, the recognized MRO defects are significantly important in both cavitation and shear transformation, which are two intrinsic deformation modes of MGs.

2. Simulation and methods

The MD simulations are carried out with the open source code LAMMPS [44]. A simple binary MG $Zr_{50}Cu_{50}$ is selected as the model material. We employ the Finnis-Sinclair type interatomic potential with parameters given by Mendelev et al. [45] to describe the interactions in the Zr–Cu system. Glass samples are prepared via a melting-and-quenching process [46]. Simulations are performed in the constant number of particles, pressure, and temperature (*NPT*) ensembles, the time step for integration is chosen to be 1 fs, and three-dimensional periodic boundary conditions with ambient pressure are applied. The initial system with ~55,000 atoms is a fcc lattice in a cubic shape, with the sites randomly occupied by Zr and Cu atoms in accordance with the nominal composition. With different random seeds, several samples with different initial configurations are obtained. For each sample, temperature is raised gradually from 1 K to 2500 K, equilibrates for 100 ps and cools down to 300 K, with the same heating and cooling rate of 5 K/ps. After a further relaxation for 100 ps, glass samples with dimensions of ~$10 \times 10 \times 10$ nm^3 are prepared. For simulations of cavitation instability, all the samples are subjected to uniform hydrostatic tension with the volumetric stain rate of ~6×10^{-4} ps^{-1}. The loading is carried out without temperature control, to capture temperature effects related to plasticity [47].

To analyze the atomic structures of MGs, the Voronoi tessellation method is employed [48]. With this method, each atom is indexed with the Voronoi indices $< n_3, n_4, n_5, n_6, \ldots >$, where n_3, n_4, n_5 and n_6 represent the number of triangles, tetragons, pentagons and hexagons on the Voronoi polyhedron, respectively. And the structure feature of the central atom and its nearest neighbors can be characterized.

3. Results and discussions

3.1. Micro-structure evolution during cavitation instability

Fig. 1 shows the evolution of atomic configuration of one sample (denoted as S1) before a void is nucleated with colors indicating the normalized local atomic number density ρ/ρ_{mean}. The red color represents lower values of ρ/ρ_{mean}, while the blue color represents higher values. Atomic density fluctuation is clearly observed in this CuZr MG. As the applied tensile volumetric strain increases, a void is nucleated in the sample. It should be noted that the void is not nucleated in a region with the lowest density (or the highest free volume content), but in a region with relatively lower density as shown in Fig. 1(a). Just before void nucleation, the density begins to decrease a lot at the nucleation site. As free volume is believed to play an important role during the void nucleation process [46,49], this phenomenon is beyond our expectation. It implies that not only the free volume content but also the atomic packing has significant influence.

Fig. 2 show the change in population of polyhedra with increasing volumetric strain before void nucleation. Different types of polyhedra are sorted according to their population from large to small. Then the former 50 types are divided into 5 groups, each containing 10 types, and other types are counted in the rest group. As shown in Fig. 2, in the initial configuration, the total fraction of the first group which contains the top 10 major polyhedra approaches 40%, while the rest 60% is the fraction of all the other groups. With increasing the volumetric strain, the fraction of major polyhedra decreases, corresponding to the increase in the fraction of minor polyhedra with the same amplitude. The larger populations the polyhedra have, the more their fraction decrease. In the first group, most polyhedra are stable or solid-like clusters with high density of fivefold bonds. Such as <0, 0, 12, 0>, <0, 2, 8, 2>, <0, 3, 6, 4>, <0, 1, 10, 2>, <0, 2, 8, 1> and <0, 3, 6, 3> polyhedra, they are usually Cu-centered icosahedral-like clusters which lead to dense atomic packing and slow dynamics [50–52]. And <0, 2, 8, 5>, <0, 1, 10, 4>, <0, 2, 8, 6> polyhedra, which are usually Zr-centered clusters, are also stable clusters [51,52]. In contrast, most of the minor polyhedra are usually liquid-like clusters fragmented with high disclination density [4]. Thus, the variety in population of polyhedra implies that the atomic structure of the sample becomes more liquid-like under tensile pressure. As liquid-like clusters are more unstable, atom rearrangement easily occurs. This feature is expected to benefit void nucleation.

Are voids prone to nucleate in the liquid-like regions in MGs? To answer this question, we propose a simple parameter to distinguish the liquid-like regions and the solid-like regions in the amorphous structure, as follows:

$$F_n = \frac{N_n}{N_{cut-off}}, \tag{1}$$

where F_n is the fraction of the top n major polyhedra in the local structural environment, $N_{cut-off}$ is the total number of atoms within the cutoff distance, and N_n is the number of the top n major polyhedra within the cutoff distance. It is known that MG would tend to maximize its favourable SROs, which elevates the stiffness and slows down the relaxation dynamics, and leads to more ordered configurations [53]. For a well relaxed MG, the major polyhedra are just the most favourable polyhedra in MGs. Thus, the main difference of atomic structure between the solid-like regions and the liquid-like regions can be attributed to the different fraction of major polyhedra. For a larger F_n, it means that the local structural environment is dominated by the most favourable polyhedra and is dense packing in SRO.

For the CuZr MG in this letter, a value of $n = 10$ and a cutoff distance of 7.6 Å are used to obtain F_n. Fig. 3 illustrates the distribution of solid-like and liquid-like regions in S1. The red color represents lower values of F_n, while the blue color represents higher values. Liquid-like regions and solid-like regions of nanometer scale are clearly distinguished. As volumetric strain increases, all regions become to be more liquid-like gradually. Beyond our expectation, void nucleation occurs at a solid-like region in the initial configuration. Just before the void is nucleated, the region turns to be liquid-like.

Now the features of nucleation site in sample S1 can be concluded: it is located at a region with relatively lower density, but with relatively higher value of F_n. To find the common features, cavitation instability in several other samples are explored. Fig. 4 shows the initial configuration of each sample with green circles denoting the nucleation sites. It is found that there is a little

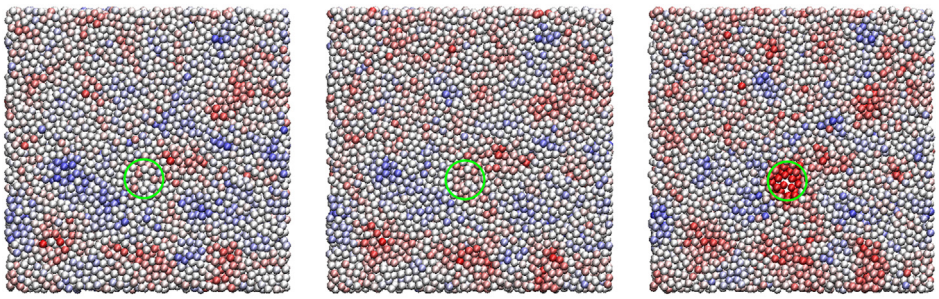

Fig. 1. Evolution of atomic configurations before void nucleation in S1 at different volumetric strain ε_v. The slice with thickness of 1 nm is taken for the illustration. The color indicates the normalized local atomic number density ρ/ρ_{mean}.

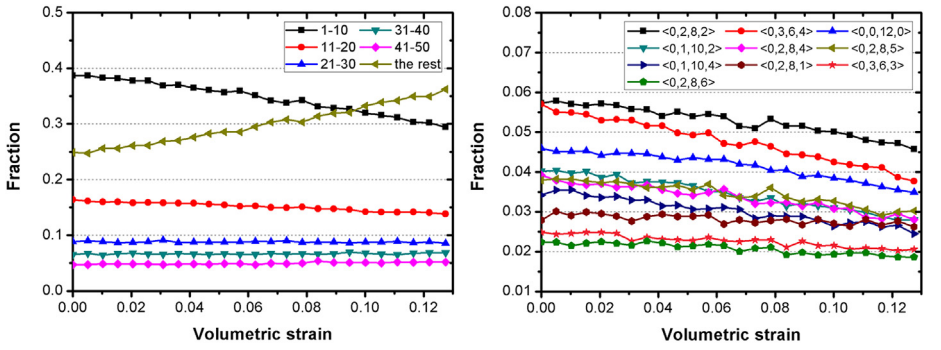

Fig. 2. Change in population of major polyhedra as a function of volumetric strain in S1.

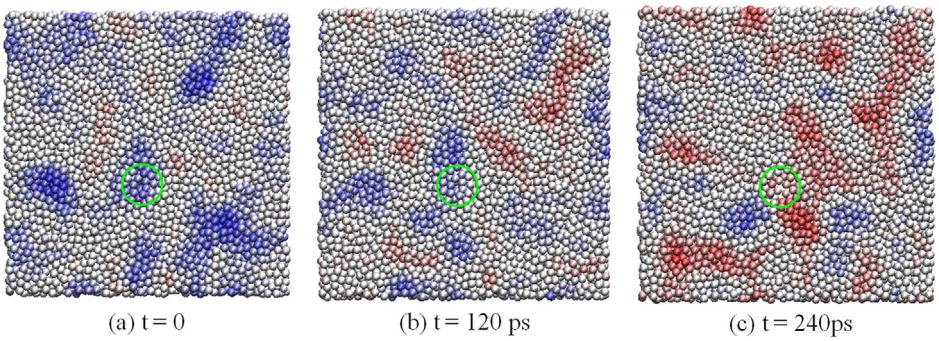

Fig. 3. Distribution of solid-like and liquid-like regions in atomic structure of S1 with increasing volumetric strain. The same slice with thickness of 1 nm is taken for the illustration. The colors indicate the value of F_n.

difference between some of the results. As the density becomes lower at the nucleation sites, a lower F_n is required (see S2 and S4).

3.2. MRO defects and their effect of on cavitation

What is the nature behind the phenomenon? Based on the concept of free volume, we think that the total free volume content (denoted as v_t) is composed of two parts, as follows:

$$v_t = v_{SR} + v_{MR}, \tag{2}$$

where v_{SR} is the free volume content in an atomic cluster, determined by atomic packing in SRO; v_{MR} is the free volume content among atomic clusters, corresponding to the cluster packing on medium range. Our results imply that a higher v_t and a lower v_{SR} benefits void nucleation. Thus, it is indicated that voids are prone to nucleation in the region where atomic clusters are loose packing on medium range.

To further study the influence of cluster packing on the void nucleation, evolution of Cu-centered clusters around the nucleation site in S1 is examined as shown in Fig. 5. In the initial configuration shown in Fig. 5(a), clusters around the nucleation site exhibit icosahedral-like ordering. Some of them connect each other with common vertex forming MROs. Although atoms are dense packing in icosahedral-like SRO, the atomic clusters are somewhat loose packing in medium range. Cavities (empty spaces or a relatively large amount of free volume) can be found among atomic clusters, and a boundary, across which the icosahedral-like clusters are not connected, exists between MROs. With increasing applied volumetric strain, there is no apparent change in SRO. The full

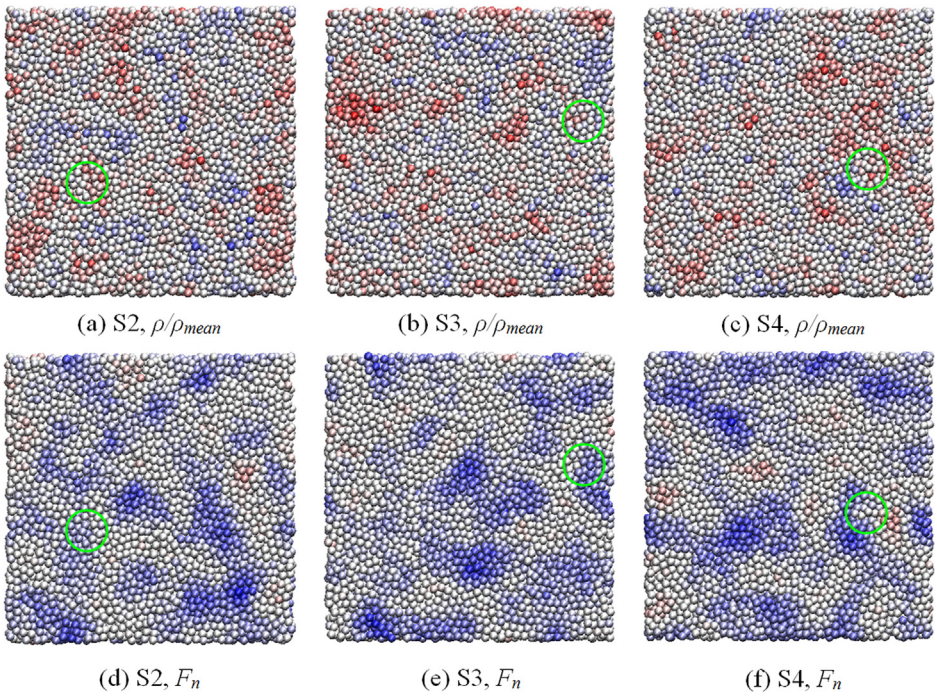

Fig. 4. The initial configurations of several other samples with green circles denoting the nucleation sites. The colors indicate the normalized local atomic number density ρ/ρ_{mean} in (a)–(c), and the value of F_n in (d)–(f). (For interpretation of the references to colour in this figure legend, the reader is referred to the web version of this article.)

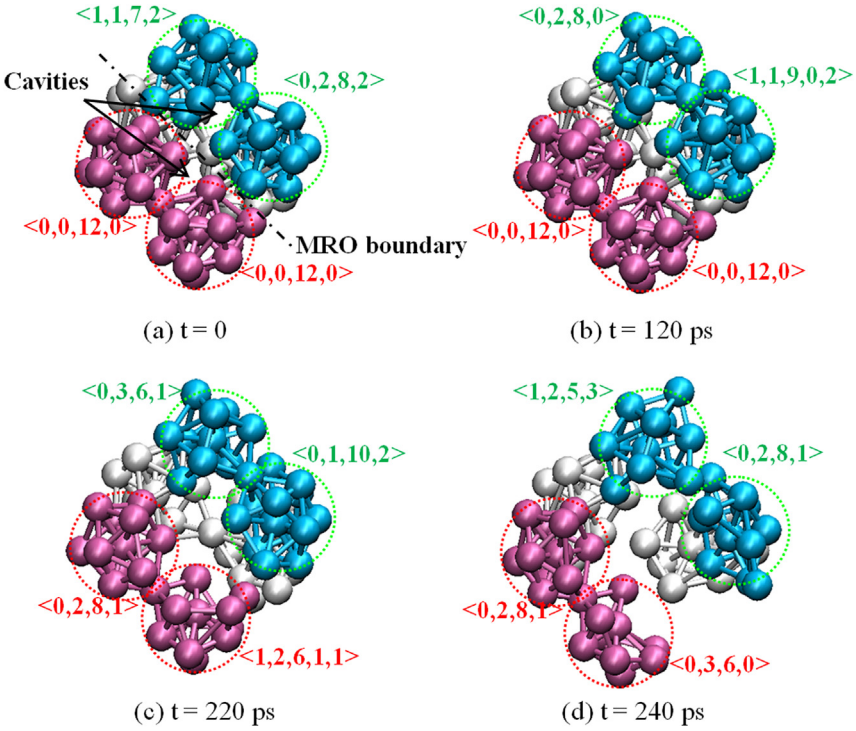

Fig. 5. Evolution of Cu-centered clusters around the void nucleation site.

icosahedral clusters remain stable, and other clusters are distorted slightly. However, the medium-range structures are gradually changed. As the SRO clusters separate from each other, free volume tends to accumulate at the sites of empty spaces, leading to the growth of the cavities. And the spacing of the boundary between MROs enlarges. During the process, MRO plays a role as confinement, for the connection between SRO clusters tends to prevent the separation. As the tensile pressure approaches to a critical value for cavitation instability, the confinement is broken and all the atomic clusters cannot keep stable anymore, they are severely distorted. Cleavage of atomic clusters occurs along the MRO boundary and coalescence of cavities takes place. Thus, a void

is nucleated.

Based on the evolution of atomic clusters, it is obvious that the cavities and MRO boundaries play important roles during the void nucleation process. They are heterogeneities on medium range, and can be interpreted as intrinsic structural defects in MGs. On one hand, cavities among polyhedra are natural sites for free volume clustering. They can be interpreted as point defects in MGs, analogous to the vacancies in crystalline materials. In fact, there may be no regularly spaced cavities in MGs, for the atomic structure is usually densely packed and atomic clusters can be distorted to be accommodated in the overall structure [53]. We think that just in the region where the atomic clusters are too stable to be distorted and the cluster packing is loose in medium range, cavities (or empty spaces) can be left behind. On the other hand, MRO boundaries are the natural weak linkage of backbone structures in MGs. They can be viewed as planer defects, analogous to grain boundaries in polycrystalline materials. As connection of the icosahedral-like clusters forms strong network in MGs, it is difficult to break the network. The MRO boundary provide a cleavage or sliding path to separate one part of network from another.

3.3. Effect on shear transformation

Since the cavities and MRO boundaries are thought to be the intrinsic defects in MGs, it is expected that they not only play key roles in the cavitation instability, but also in other deformation behaviors responding to the external stimuli, e. g, the shear transformation. To demonstrate it, additional simulations on compression of the same sample S1 are carried out. Compressive strain is applied along the Y axis with a strain rate of 0.25 ns^{-1} at $T = 300$ K and the period boundary conditions on three dimensions [8]. Fig. 6(a) and (b) illustrate the atomic configuration of the same slice at different magnitude of strain. Plastic deformation is identified by the nonaffine displacement D^2_{min} proposed by Falk and Langer [54] with a time interval of $\Delta t = 40$ ps. As compressive strain increases, the region with MRO defects (denoted by green circles) undergoes relatively larger plastic deformation, although there are plenty of stable icosahedral-like clusters. Details of atomic clusters evolution around the site is shown in Fig. 6(c) and (d). At a lower stain of 0.05, shear transformation seems to occur on short range, which is achieved by slightly distortion of atomic clusters, such as <0, 0, 12, 0>, <1, 1, 7, 2> in Fig. 6(c). And the cavities play a role like free volume which decreases free energy barrier for rearrangement [30,55]. However, at a higher strain of 0.10, the shear transformation is closely related to the relative motion of atomic clusters on medium range, which is mediated by MRO defects. This phenomenon is similar to the grain boundary sliding behavior of polycrystals which involves the relative motion of two neighboring crystallites. It is clear that the cavities provide empty space for the clusters up and down to squeeze into, and the MRO boundary serves as a sliding plane.

4. Conclusion

In summary, via molecular dynamics simulations of cavitation instability in an CuZr MG, the atomic structural evolution process is studied. Although the number of simulations is limited, our preliminary results show that the nucleation sites are located at

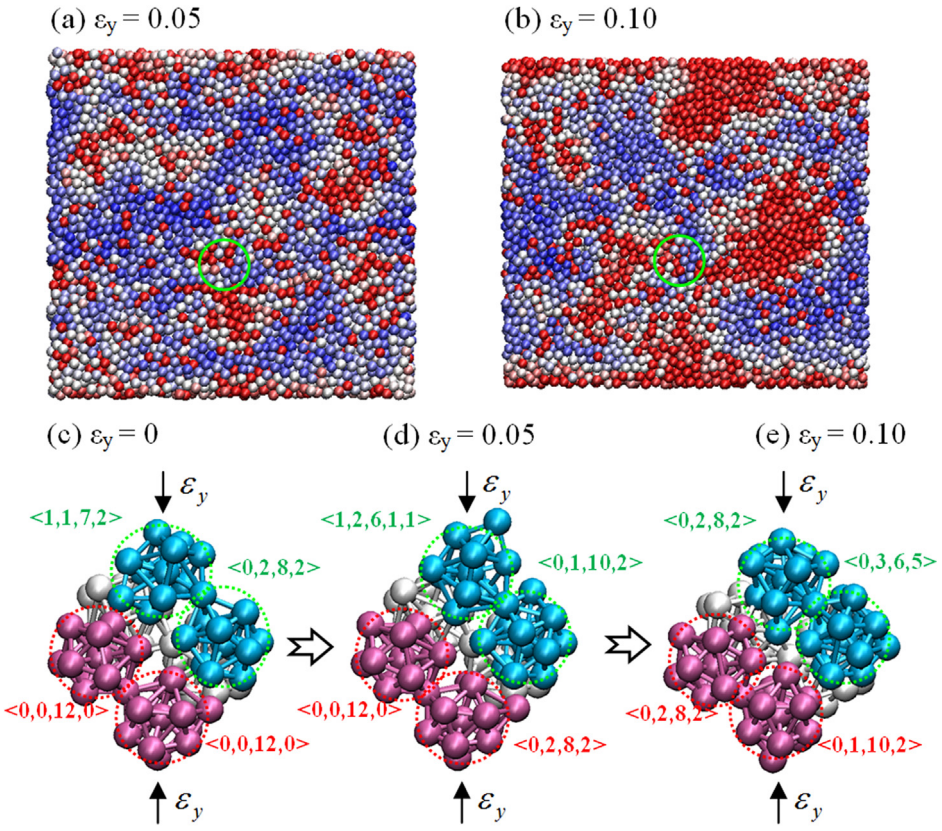

Fig. 6. Deformation of sample S1 under compressive loading. Atomic configurations of the same slice are illustrated at the strain of (a) 5% and (b) 10%. The colors indicate values of the nonaffine displacement D^2_{min} when $\Delta t = 40$ ps. The red color represents higher values, while the blue color represents lower values. Details of atomic clusters evolution in the region with MRO defects (denoted by green circles) is shown in (c), (d) and (e). (For interpretation of the references to colour in this figure legend, the reader is referred to the web version of this article.)

regions where the atomic structures are loose packing on medium range. Detailed investigation of atomic clusters around the nucleation site shows that cavities and MRO boundaries are intrinsic structural defects on medium range in MGs. They play important roles in void nucleation process. Under external tensile pressure, free volume is prone to accumulation at the sites, which induces growth of the cavities. The cleavage of MRO boundaries finally leads to coalescence of cavities, and then a void is nucleated. Further investigation on deformation of the MG under compressive loading shows that motion of atomic clusters on medium range is mediated by the defects, which leads to a shear transformation event. We therefore propose two kinds of MRO defects, i.e., cavity and boundary, between the SRO atomic clusters in MGs. They play critical roles in both cavitation and shear transformation of amorphous solids.

Acknowledgment

Financial support was from the NSFC (Grants Nos.: 11402245, 11272328 and 11472287), the National Basic Research Program of China (Grants No. 2012CB937500), the Foundation of the China Academy of Engineering Physics (Grants No. 2014B0201024), and the key subject “Computational Solid Mechanics” of the China Academy of Engineering Physics.

References

[1] D.R. Curran, L. Seaman, D.A. Shockey, Dynamic failure of solids, Phys. Rep. 147 (1987), 253–388.
[2] A.L. Greer, Metallic glasses, Science 267 (1995) 1947–1953.
[3] W.H. Wang, C. Dong, C.H. Shek, Bulk metallic glasses, Mater. Sci. Eng. R. 44 (2004) 45–89.
[4] Y.Q. Cheng, E. Ma, Atomic-level structure and structure–property relationship in metallic glasses, Prog. Mater. Sci. 56 (2011) 379–473.
[5] T. Egami, Atomic level stresses, Prog. Mater. Sci. 56 (2011) 637–653.
[6] W.H. Wang, Y. Yang, T.G. Nieh, C.T. Liu, On the source of plastic flow in metallic glasses: concepts and models, Intermetallics 67 (2015) 81–86.
[7] Y.Z. Guo, M. Li, Atomistic simulation of a NiZr model metallic glass under hydrostatic pressure, Appl. Phys. Lett. 94 (2009) 051901.
[8] H.L. Peng, M.Z. Li, W.H. Wang, Structural signature of plastic deformation in metallic glasses, Phys. Rev. Lett. 106 (2011) 135503.
[9] H.L. Peng, M.Z. Li, W.H. Wang, C.-Z. Wang, K.M. Ho, Effect of local structures and atomic packing on glass forming ability in Cu_XZr_{100-X} metallic glasses, Appl. Phys. Lett. 96 (2010) 021901.
[10] W.D. Li, H. Bei, Y. Tong, W. Dmowski, Y.F. Gao, Structural heterogeneity induced plasticity in bulk metallic glasses: from well-relaxed fragile glass to metal-like behavior, Appl. Phys. Lett. 103 (2013) 171910.
[11] W.D. Li, Y.F. Gao, H. Bei, On the correlation between microscopic structural heterogeneity and embrittlement behavior in metallic glasses, Sci. Rep. 5 (2015) 14786.
[12] J.D. Bernal, Geometry of the structure of monatomic liquids, Nature 185 (1960) 68–70.
[13] M. Wakeda, Y. Shibutani, S. Ogata, J. Park, Relationship between local geometrical factors and mechanical properties for Cu–Zr amorphous alloys, Intermetallics 15 (2007) 139–144.
[14] P.F. Damasceno, M. Engel, S.C. Glotzter, Predictive self-assembly of polyhedra into complex structures, Science 337 (2013) 453–457.
[15] D.B. Miracle, A structural model for metallic glasses, Nat. Mater. 3 (2004) 697–702.
[16] F.C. Frank, Supercooling of liquids, Proc. R. Soc. Lond. 215 (1952) 43–46.
[17] Y.Q. Cheng, H.W. Sheng, E. Ma, Relationship between structure, dynamics, and mechanical properties in metallic glass-forming alloys, Phys. Rev. B 78 (2008) 014207.
[18] A. Hirata, L.J. Kang, T. Fujita, B. Klumov, K. Matsue, M. Kotani, A.R. Yavari, M.W. Chen, Geometric frustration of Icosahedron in metallic glasses, Science 341 (2013) 376–379.
[19] P.F. Guan, T. Fujita, A. Hirata, Y.H. Liu, M.W. Chen, Structural origins of the excellent glass forming ability of $Pd_{40}Ni_{40}P_{20}$, Phys. Rev. Lett. 108 (2012) 175501.
[20] H.W. Sheng, W.K. Luo, F.M. Alamgir, J.M. Bai, E. Ma, Atomic packing and short-to-medium-range order in metallic glasses, Nature 439 (2006) 419–425.
[21] X.J. Liu, Y. Xu, X. Hui, Z.P. Lu, F. Li, G.L. Chen, J. Lu, C.T. Liu, Metallic liquids and glasses: atomic order and global packing, Phys. Rev. Lett. 105 (2010) 155501.
[22] M. Wakeda, Y. Shibutani, Icosahedral clustering with medium-range order and local elastic properties of amorphous metals, Acta Mater. 58 (2010) 3963–3969.
[23] E. Ma, J. Ding, Tailoring structural inhomogeneities in metallic glasses to enable tensile ductility at room temperature, Mater. Today (2016) in press, Available online April 30th, 2016, http://dx.doi.org/10.1016/j.mattod.2016.04.001.
[24] W.K. Luo, H.W. Sheng, E. Ma, Pair correlation functions and structural building schemes in amorphous alloys, Appl. Phys. Lett. 89 (2006) 131927.
[25] Y. Zhang, F. Zhang, C.Z. Wang, M.I. Mendelev, M.J. Kramer, K.M. Ho, Cooling rates dependence of medium-range order development in $Cu_{64.5}Zr_{35.5}$ metallic glass, Phys. Rev. B 91 (2015) 064105.
[26] X.J. Liu, Y. Xu, Z.P. Lu, X. Hui, G.L. Chen, G.P. Zheng, C.T. Liu, Atomic packing symmetry in the metallic liquid and glass states, Acta Mater. 59 (2011) 6480–6488.
[27] Z.W. Wu, M.Z. Li, W.H. Wang, K.X. Liu, Correlation between structural relaxation and connectivity of icosahedral clusters in CuZr metallic glass-forming liquids, Phys. Rev. B 88 (2013) 054202.
[28] D. Ma, A.D. Stoica, X.L. Wang, Power-law scaling and fractal nature of medium-range order in metallic glasses, Nat. Mater. 8 (2009), 1476–4660.
[29] D.Z. Chen, C.Y. Shi, Q. An, Q.S. Zeng, W.L. Mao, W.A. Goddard, J.R. Greer, Fractal atomic-level percolation in metallic glasses, Science 349 (2015) 1306–1310.
[30] F. Spaepen, A microscopic mechanism for steady state inhomogeneous flow in metallic glasses, Acta Metall. 25 (1977) 407–415.
[31] D.R. Nelson, Order, frustration, and defects in liquids and glasses, Phys. Rev. B 28 (1983) 5515–5535.
[32] M.Q. Jiang, L.H. Dai, On the origin of shear banding instability in metallic glasses, J. Mech. Phys. Solids 57 (2009) 1267–1292.
[33] R. Narasimhan, P. Tandaiya, I. Singh, R.L. Narayan, Fracture in metallic glasses: mechanics and mechanisms, Int. J. Fract. 191 (2015) 53–75.
[34] M.M. Trexler, N.N. Thadhani, Mechanical properties of bulk metallic glasses, Prog. Mater. Sci. 55 (2010) 759–839.
[35] F. Faupel, W. Frank, M.P. Macht, H. Mehrer, V. Naundorf, K. Ratzke, H.R. Schober, S.K. Sharma, H. Teichler, Diffusion in metallic glasses and supercooled melts, Rev. Mod. Phys. 75 (2003) 237–280.
[36] S.X. Song, T.G. Niehb, Direct measurements of shear band propagation in metallic glasses - an overview, Intermetallics 19 (2011) 1968–1977.
[37] Z.Y. Liu, Y. Yang, C.T. Liu, Yielding and shear banding of metallic glasses, Acta Mater. 61 (2013) 5928–5936.
[38] F. Shimizu, S. Ogata, J. Li, Yield point of metallic glass, Acta Mater. 54 (2006) 4293–4298.
[39] Y.W. Wang, M. Li, J.W. Xu, Toughen and harden metallic glass through designing statistical heterogeneity, Scr. Mater. 113 (2016) 10–13.
[40] Y. Fan, T. Iwawaki, T. Egami, How thermally activated deformation starts in metallic glass, Nat. Commun. 5 (2014) 5083.
[41] S. Karmakar, A. Lemaitre, E. Lerner, I. Procaccia, Predicting plastic flow events in athermal shear-strained amorphous solids, Phys. Rev. Lett. 104 (2010) 215502.
[42] Y. Fan, T. Iwashita, T. Egami, Crossover from localized to cascade relaxations in metallic glasses, Phys. Rev. Lett. 115 (2015) 045501.
[43] P. Guan, S. Lu, M.J.B. Spector, P.K. Valavala, M.L. Falk, Cavitation in amorphous solids, Phys. Rev. Lett. 110 (2013) 185502.
[44] S. Plimpton, Fast parallel algorithms for short-range molecular dynamics, J. Comput. Phys. 117 (1995) 1–19.
[45] M.I. Mendelev, D.J. Sordelet, M.J. Kramer, Using atomistic computer simulations to analyze x-ray diffraction data from metallic glasses, J. Appl. Phys. 102 (2007) 043501.
[46] P. Murali, T. Guo, Y. Zhang, R. Narasimhan, Y. Li, H. Gao, Atomic scale fluctuations govern brittle fracture and cavitation behavior in metallic glasses, Phys. Rev. Lett. 107 (2011) 215501.
[47] E.M. Bringa, S. Traiviratana, M.A. Meyers, Void initiation in fcc metals: effect of loading orientation and nanocrystalline effects, Acta Mater. 58 (2010) 4458–4477.
[48] G. Voronoi, New parametric applications concerning the theory of quadratic forms – second announcement, J. Reine Angew. Math. 134 (1908) 198–287.
[49] X. Huang, Z. Ling, H.S. Zhang, J. Ma, L.H. Dai, How does spallation microdamage nucleate in bulk amorphous alloys under shock loading? J. Appl. Phys. 110 (2011) 103519.
[50] F. Li, X.J. Liu, Z.P. Lu, Atomic structural evolution during glass formation of a Cu-Zr binary metallic glass, Comput. Mater. Sci. 85 (2014) 147–153.
[51] H.L. Peng, M.Z. Li, W.H. Wang, C.Z. Wang, K.M. Ho, Effect of local structures and atomic packing on glass forming ability in Cu_xZr_{100-x} metallic glasses, Appl. Phys. Lett. 96 (2010) 021901.
[52] J. Ding, S. Patinet, M.L. Falk, Y.Q. Cheng, E. Ma, Soft spots and their structural signature in a metallic glass, Proc. Natl. Acad. Sci. U. S. A. 111 (2014) 14053.
[53] E. Ma, Tuning order in disorder, Nat. Mater. 14 (2015) 547–552.
[54] M.L. Falk, J.S. Langer, Dynamics of viscoplastic deformation in amorphous solids, Phys. Rev. E 57 (1998) 7192–7205.
[55] A.S. Argon, Plastic-deformation in metallic glasses, Acta Metall. 27 (1979) 47–58.